

# A groundwater tracing investigation as an aid of locating groundwater monitoring stations on the Mitchell Plain of southern Indiana

Wanfang Zhou · Barry F. Beck · Arthur J. Pettit · Brad J. Stephenson

**Abstract** A groundwater tracing study was conducted on the Mitchell Plain of southern Indiana to aid in the design of a karst groundwater monitoring program for a proposed landfill facility. Fluorescein and rhodamine WT dyes were introduced into sinkholes at the project site. On-site fluorometric analyses and concentration-dependent sampling were utilized at springs and a local stream for data resolution while minimizing delays between tracing events. As a result of this investigation, springs including a submerged spring that drain groundwater from the site have been identified and two groundwater monitoring stations have been established. The submerged spring was discovered in the streambed at intersections between prominent joints and solution-enlarged bedding-plane partings. It could not have been identified readily during a typical karst hydrogeologic inventory, nor would it have been detected by analyzing charcoal dye receptors with a spectrofluorometer.

**Keywords** Dye tracing · Karst · Groundwater monitoring

## Introduction

The study site is located on the eastern slope of a small stream valley, which is entrenched into the Mitchell Plain of southern Indiana. The Mitchell Plain is a 2,900-km<sup>2</sup> limestone plateau characterized by an abundance of underground drainage and a lack of streams on the land surface (Powell 1961; McConnell and Horn 1972; Lehmann 1975). Physiographically, it is a subunit of the Highland Rim Section of the Interior Low Plateaus Province (Malott 1919; Fenneman 1938) (Fig. 1). It extends southward into Kentucky as the Pennyroyal Plateau; to the north, it is covered with a thick blanket of Pleistocene till (McConnell and Horn 1972; Palmer and Palmer 1975). A sinkhole plain occupies the westernmost 30% of the Mitchell Plain (Palmer and Palmer 1975).

Sinkholes and dendritic cave systems have developed in response to the dissection of the Mitchell Plain by entrenching streams (Palmer and Palmer 1975). Powell (1961) and Ash (1980) summarize several of the prevailing theories regarding cave development beneath the Mitchell Plain. Most known caves lie within the massive, prominently jointed Salem Limestone, while the majority of sinkholes occur in the thinner beds of the overlying St. Louis Limestone (Palmer and Palmer 1975; Johnson and Gomez 1994). The materials overlying the St. Louis Limestone consist of a clay-rich, cherty residuum from the weathering of the underlying limestone (Powell 1961; Palmer and Palmer 1975), as well as colluvium, alluvium, and lacustrine material (Hall 1973, 1976a, 1976b; Olson and others 1980; Ault 1993).

Despite the relatively uniform stratigraphy throughout the Mitchell Plain, the distribution of karst features is irregular (Palmer and Palmer 1975). The sinkhole density ranges from less than 4 to 24%/km<sup>2</sup> (Ruhe 1977). In the most highly karstified portions of the plain, more than 40 sinkholes occur per square kilometer on 1:24,000-scale topographic maps with a 3 m contour interval. However, field studies have shown that the actual density is more than ten times greater. Malott (1945) surveyed 1,022 sinkholes in a single square mile near Orleans and estimated that there may be as many as 300,000 sinkholes on the Mitchell Plain.

The large and deep sinkholes on the Mitchell Plain have formed by cave-roof collapse over large, hydrologically active cave passages (Rexroad and Gray 1979). The majority of them have formed by a combination of

Received: 27 August 2001 / Accepted: 5 November 2001  
Published online: 18 December 2001  
© Springer-Verlag 2001

W. Zhou (✉) · B.F. Beck · A.J. Pettit  
P.E. LaMoreaux & Associates, Inc.,  
106 Administration Road, Suite 4,  
Oak Ridge, Tennessee 37830, USA  
E-mail: wzhou@pela-tenn.com  
Tel.: +1-865-4837483  
Fax: +1-865-4837639

B.J. Stephenson  
ARCADIS Geraghty & Miller Inc.,  
97 Midway Lane, Oak Ridge,  
TN 37830, USA

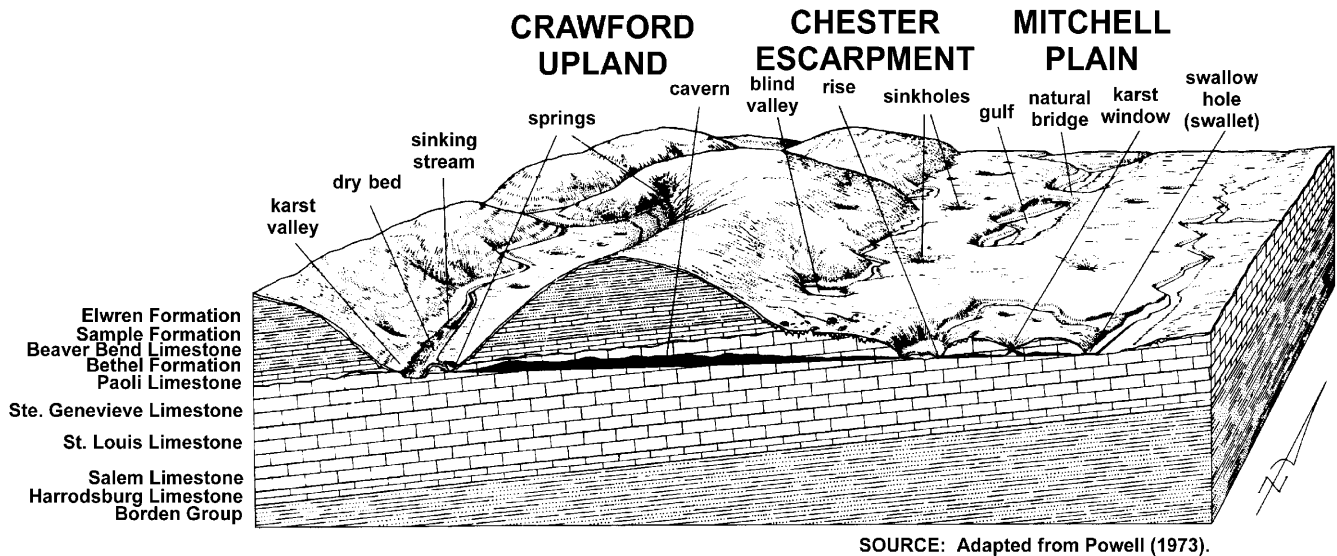


**Fig. 1**  
Idealized karst geomorphology of the Mitchell Plain area

limestone solution and cover-sediment erosion. Cover-collapse sinkholes tend to develop over plugged drainage conduits of existing sinkhole basins (Frushour and others 1997; Powell and others 1997).

Seven sinkholes occurred in the vicinity of the study site and they are labeled as A through G in Fig. 2. Sinkholes A, B, C, D, and E are on the valley slope, generally northwest of the site. None of these sinkholes show any evidence of being formed by cave-roof collapse. Sinkholes A, B, C, and E all capture surface drainage and transmit it underground through small openings at the bottom. When first examined the bottom of sinkhole D was choked with debris and sediment, and there was no outlet visible. Excavation with a backhoe intercepted a natural soil cavity. Sinkhole F is larger than the aforementioned depressions and is immediately east of the site on the upland. A small drainage channel crosses the broad bottom of this sinkhole and sinks into an open hole near the southern slope. Sinkhole G is south of the site. The closed depression on the site map is one third of what was formerly a larger sinkhole. The construction of a road bisected this sinkhole, and it is probable that the filling for the road base covered the original drain. At present, water ponds in sinkhole G and slowly drains by seeping into the soil.

A number of small springs, such as QRS, QNS, and QBS, discharge groundwater to a local stream-RLB along the base of the valley slope just west of the site. QNS is located at the head of a short, steep valley, whereas QRS and QBS emerge from small openings in the valley floor. The discharge of the springs is small, even after rainfall; however, they respond very quickly to recharge. In addition to the springs and sinkholes, other karst features identified in the vicinity of the site include sinking streams, caves, and seeps.

State and Federal regulations have established restrictions for the location of hazardous waste and municipal, solid waste landfills in such a terrain (Hughes and others 1994).

Regulations require the owners/operators to demonstrate that the hydrogeology has been adequately characterized, the site is not subject to destabilizing events, and that the locations for monitoring wells have been properly selected. An area characterized by karst does not automatically declare it to be unsuitable for siting waste disposal facilities or other engineered works (Hatheway 1996). However, a wide range of potential complexities in the karst system mandates application of special and advanced techniques to determine the feasibility of a specific site for a landfill facility. At this location, the integrity of the potential landfill site was investigated by earth resistivity imaging (Zhou and others 2000) and natural potential measurements (Zhou and others 1999), in addition to the more conventional karst inventory, fracture trace analysis, satellite image interpretation, and exploratory boreholes. This present paper shows how on-site fluorometric analysis of fluorescent dyes and a concentration-dependent sampling strategy helped with the establishment of the groundwater monitoring stations.

## Tracing tests in karst aquifers

Groundwater flow in karst aquifers such as this is normally conduit or fracture dominated. The flow processes are complex due to the typically extreme heterogeneity and anisotropy. As a result, karst aquifers are often not amenable to such conventional groundwater investigative techniques as potentiometric surface mapping and aquifer testing, especially at shallow depth. It is not uncommon for groundwater flow in karst aquifers to be very rapid, appear to be traveling parallel to equipotential lines, or appear to be traveling against the regional hydraulic gradient. Some karst aquifers have demonstrated large-scale divergent radial flow of groundwater via discrete conduits. Other problems such as high-level overflow routes and large storm-related variability in water quality further complicate karst aquifers.

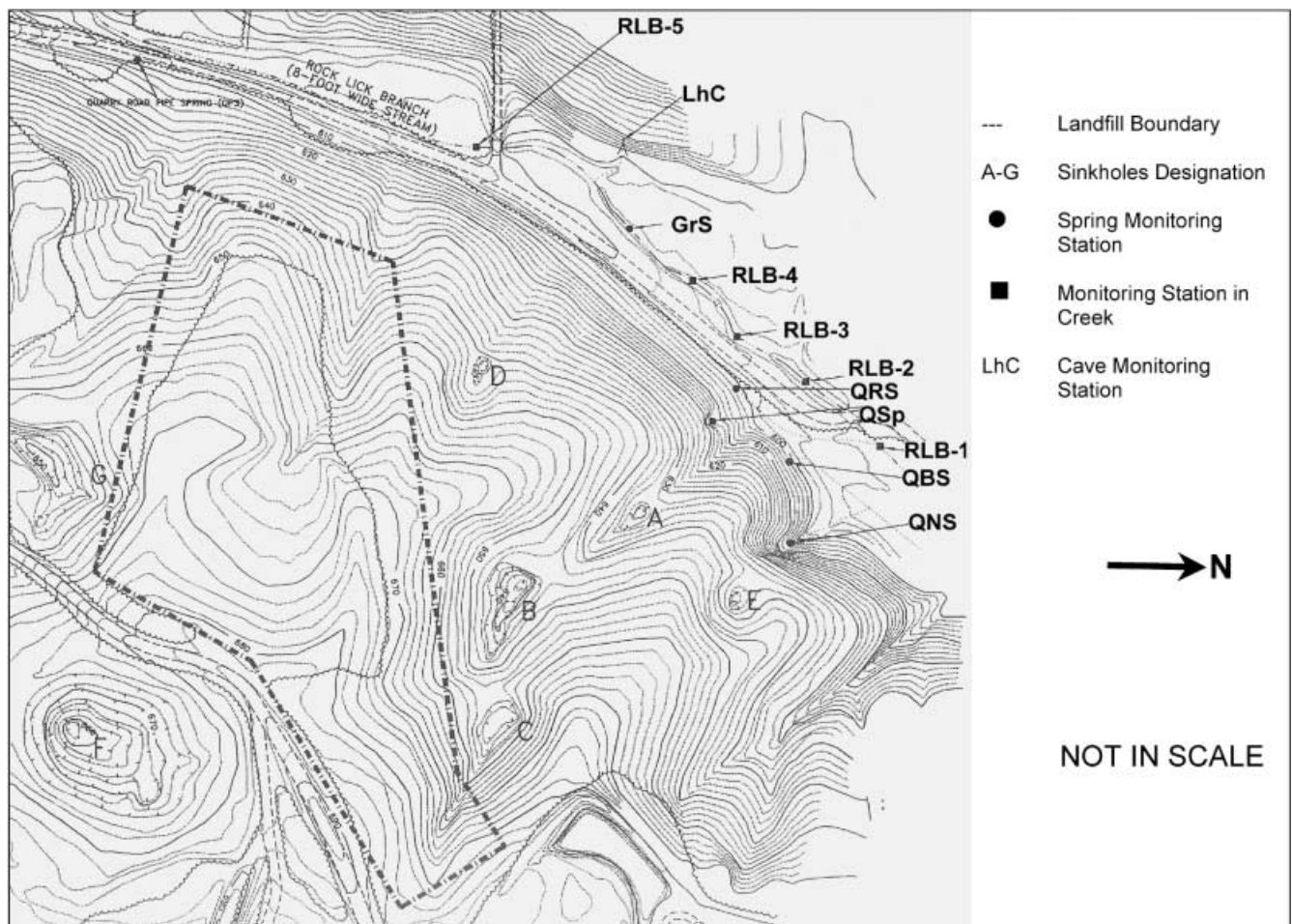


**Fig. 2**  
Site map

Groundwater tracing studies using fluorescent dyes are a commonly accepted diagnostic technique to determine flow connection between accessible input and output points, to delineate karst drainage basins, and to investigate the flow characteristics of karst aquifers. Many groundwater problems, such as source water (well- or spring-head) protection investigations, can benefit from simple point-to-point groundwater tracing studies (Eckenfelder 1996). Other groundwater problems, such as pollution migration from hazardous waste landfills, may demand more sophisticated, quantitative groundwater tracing studies because of the need to better define subsurface hydraulic and transport processes (Quinlan 1986). Quantitative or semi-quantitative tracing requires reliable time-concentration data to define tracer breakthrough curves, which also lends credibility to a qualitative trace. When fluorometric dye analysis is used, quantitative tracing provides a possible means to obtain statistically reliable results without discoloring the spring water or any surface water bodies. The breakthrough curves can be interpreted to estimate total tracer recovery, mean residence time, mean velocity, longitudinal dispersion, and maximum volume of aquifer conduits (Rainwater and others 1987; Kass 1998) and have been effectively used to

evaluate the hydraulic processes of dispersion, divergence, convergence, dilution, and storage (Broermann and others 1997; Zhou 2000). This improvement in karst aquifer assessment efforts translates into better groundwater resource management, groundwater monitoring designs, and groundwater remediation.

A dye breakthrough curve is theoretically determined by the conduit network pattern (Brown and Wigley 1969; Atkinson and Smart 1981; Smart and Ford 1982), the flow characteristics of the aquifer (Jones 1984; Quinlan 1990), and the adsorption/dispersion properties of the tracer (Kasnavia and others 1998). In practice, however, it is also impacted by the sampling frequency. Sampling with insufficient frequency may produce misleading breakthrough curves, a problem known as aliasing (Quinlan and Alexander 1987; Currens 1995), or lead to a false negative detection. The main reason for the aliasing phenomenon is that the dye concentration in conduit-dominated karst aquifers often varies dramatically with time, especially when the movement of the injected dye is driven by runoff events. Sampling with regular intervals is unlikely to characterize the dye breakthrough curve unless the frequency is very intense. Flow-dependent sampling may improve the dye trace results but may also result in a less representative breakthrough curve because of the phase difference between the spring hydrograph and breakthrough curve (Ryan and Meiman 1995; Stephenson and others 1999).

Recently, several studies have proposed the use of linear transfer (kernel) functions to describe the breakthrough curve patterns (Dreiss 1989; Wicks and Hoke 2000). If assumptions of linearity and time invariance are made, the observed fluctuations in the chemical composition of spring flow can be analyzed by treating the karst conduit system as a linear filter that transfers input stimuli into output responses. In tracer tests, where the input and output series are the mass rate of solute entering and leaving the system, respectively, the transfer function represents both the residence time distribution of the solute in the system, and the probability distribution of solute travel times. With complete mixing and conservative tracers, the shape of breakthrough curves often closely match a two-parameter gamma function, given by:

$$f(x) = \frac{x^\alpha e^{-x/\beta}}{\beta^{\alpha+1} \Gamma(\alpha+1)} \quad (1)$$

where  $0 < x < \infty$ . The parameter  $\alpha$  is a dimensionless shape factor, and  $\beta$  is a positive scale factor having the same unit as  $x$  and controlling the base length. The product of  $\alpha$  and  $\beta$  gives the value  $x$  corresponding to the apex, or the maximum value of  $f(x)$ . The distribution mean of this function is  $\beta(\alpha+1)$ , and variance is  $\beta^2(\alpha+1)$ .

The most useful feature of the gamma distribution function is that it can be conveniently used to synthesize an entire breakthrough curve by the following equation if the calculated peak concentration  $C_p$  and its associated time  $t_p$  are known (Viessman and others 1989):

$$C = C_p \left( \frac{t}{t_p} \right)^\alpha e^{\left(1 - \frac{t}{t_p}\right)\alpha} \quad (2)$$

Figure 3 shows synthetic breakthrough curves, the shape of which is impacted by both the sampling interval and the  $\alpha$  values. Obviously, the breakthrough curves obtained using a coarse sampling frequency differ significantly from those using a fine sampling frequency, especially over the period when the concentration has the greatest change. The degree of deviation is associated with the parameter  $\alpha$ , which can be used to depict flow conditions in karst aquifers. It represents the degree of mixing of injected dye with the pre-existing groundwater in the aquifer. Small values of  $\alpha$  indicate a complete mixing and that the groundwater flow tends to be diffuse, whereas large values indicate little mixing and the flow is more conduit dominated. Therefore, a "proper sampling frequency" should be site-specific and should vary with the associated flow dynamics and flow types. However, the general principle of obtaining a representative breakthrough curve, as indicated by Fig. 3, is to collect more samples when the concentration changes the most and fewer samples when the change is less dramatic – a concentration-dependent sampling strategy. This sampling strategy has been successfully applied in a quantitative tracer test at a spring in Knoxville, Tennessee (Stephenson and others 1999). Appropriate application of this sampling approach requires a progressive on-site decision on the sampling

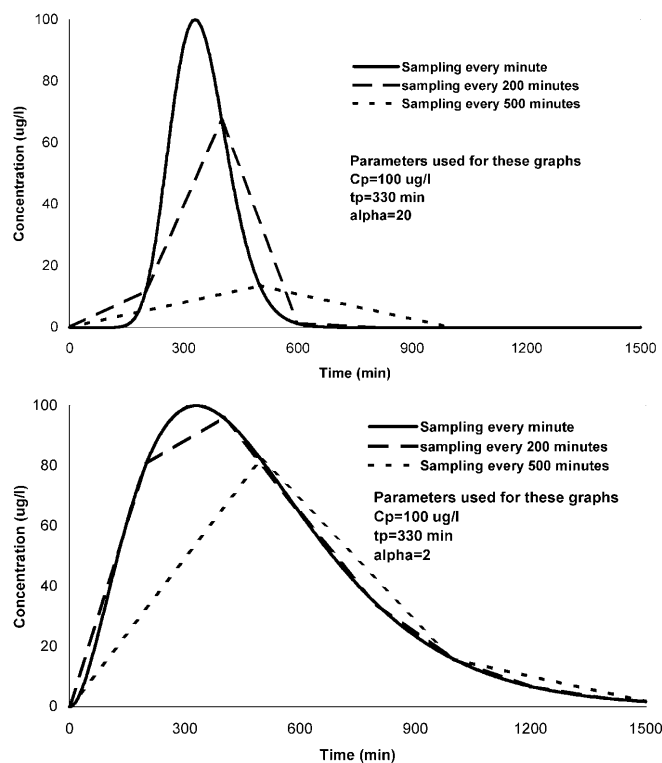


**Fig. 3** Effect of sampling frequency on breakthrough curves at different aquifers

frequency, thus an on-site instrument and experienced investigators.

## Dye injection and monitoring

Five solution sinkholes adjacent to the site (sinkholes B through F) were used to facilitate the introduction of dye into the karst aquifer. At sinkhole D, dye was inserted into a small cavity exposed by excavating with a backhoe. Dye was inserted through natural openings in sinkholes B, C, E, and F. Prior to each dye insertion, a 8 m<sup>3</sup> slug of potable water was introduced into the sinkhole. The water slugs were used to confirm that each sinkhole "drain" was permeable enough to allow the passage of dye into the subsurface. They also served to "pre-wet" the underground passages to facilitate the flow of dye. The dye was inserted with the beginning of a second 8 m<sup>3</sup> slug of water, which was followed with one or two additional slugs. The use of pre- and post-dye water insertions has proven to be an effective means for introducing dye into karst aquifers via sinkholes (Mull and others 1988). Two commonly used dyes were used during this investigation – a 50% solution of fluorescein (CI Acid Yellow 73) and a 20% solution of rhodamine WT (CI Acid Red 388).

Seven tracing tests were conducted at the investigation site. During the first four tracing tests, rhodamine WT (25 ml) was inserted into sinkholes B and C, and fluorescein was inserted into sinkholes E (25 ml) and F (100 ml). The

initial trace from sinkhole D was conducted with 25 ml of rhodamine WT. In conjunction with that activity, a second trace was conducted from sinkhole F using 1 l of fluorescein. The seventh tracing test introduced 3.8 l of rhodamine WT into sinkhole D, the results of which revealed a submerged spring at the bottom of the local stream RLB. During the tracing tests, water samples were collected manually at QRS, QBS, and QNS. Water samples were also collected at five locations (RLB-1–RLB-5) in RLB. Immediately upon collection, water samples were analyzed in the field with a filter fluorometer. The sampling frequency was adjusted according to the dye concentrations to provide higher data resolution during the rapidly rising or falling limb of the dye breakthrough curves. It also made it possible to determine when dye from one trace had been flushed from the groundwater system sufficiently to permit the next trace to be conducted. Dye samples were kept dark and refrigerated for storage. After the fieldwork, the water samples were analyzed again in the laboratory for more accurate results. Interpretations were made from the laboratory-based analyses.

## Results of tracing tests

The results of the groundwater tracing investigation are summarized in Table 1. The hydrologic connections were determined by interpretation of the dye breakthrough curves that were developed from the fluorometric analyses of water samples collected during tracing activities, as shown in Figs. 4, 5, 6, 7, 8, 9, and 10.

Because of the application of on-site fluorometric instrumentation and concentration-dependent sampling strategy, interpretation of the dye breakthrough curves is straightforward. The initial traces from sinkholes B, C, E, and F indicated that the dyes were discharged in QRS, QNS, and QBS.

The first fluorescein peak at QRS that occurred on September 24, 1997, results from insertion of dye into sinkhole F on September 23. It is a “classic” dye breakthrough curve. The connection between sinkhole F and QRS was further confirmed by inserting a larger amount of fluorescein on a later date. A minor peak on September 25 occurred almost instantaneously after the insertion of dye and water into sinkhole E. It is likely to be the result from increased hydraulic pressure rather than from the migration of dye from sinkhole E to QRS. The increased water pressure in the aquifer transported a slug of dye from the previous insertion at sinkhole F. Nevertheless, a hydraulic connection is indicated between sinkhole E and QRS. Fluorescein inserted into sinkhole F is detected at RLB-1 (Fig. 7) after being discharged from QRS.

The rhodamine WT breakthrough curve at QRS shows a double-peak feature between September 25 and 26. This could represent detection of dye from each of the two insertions – one at sinkhole C and one at sinkhole B. Alternatively, it could result solely from either dye insertion. Comparing this graph with the breakthrough curve at QNS (Fig. 5) indicates that dye from sinkhole B reached both at approximately the same time. It appears that the dye introduced into sinkhole C discharges primarily from QNS. Therefore, this double-peak feature results from the dye insertion at sinkhole B. A small rhodamine WT peak was also observed on October 16, 1997. However, detailed laboratory analysis indicated that this peak of “apparent rhodamine WT” (5.25 µg/l) is actually caused by interference from a high concentration of fluorescein (65,500 µg/l) in the water sample. In addition, the increase of turbidity of the spring water in response to stormwater runoff also generated several minor peaks.

The maximum fluorescein peak at QNS occurred on September 25, 1997, immediately after dye insertion at sinkhole E. Careful analysis of the breakthrough curve indicated another peak on September 24 with the peak

**Table 1**

Results of tracing tests. *Asterisk* not monitored. *Yes?* Hydrologic connection appears to be indicated by the data, but the data are not conclusive. *No?* Hydrologic connection does not appear to be indi-

cated by the data, but the data are not conclusive. *?* Determination regarding the existence of a hydrologic connection cannot be made based on the data

Location	Date Time	Dye Type	Volume	Hydrologic connection indicated (Yes or No)								
				Time from dye insertion to first detection (hours:minutes)								
				RLB-5	GrS	RLB-4	RLB-3	RLB-2	RLB-1	QRS	QBS	QNS
Sinkhole B	09/25/97 08:32	Rhodamine WT	25 ml	*	*	*	*	*	Yes 1:56	Yes 1:08	Yes 3:08	Yes 2:39
Sinkhole C	09/24/97 10:02	Rhodamine WT	25 ml	*	*	*	*	*	Yes 1:59	?	No	Yes 1:29
Sinkhole D	10/14/97 11:04	Rhodamine WT	25 ml	*	Yes 1:26	*	*	Yes 1:26	*	No?	No?	No?
Sinkhole D	11/18/97 12:23	Rhodamine WT	3.8 l	No	Yes 0:37	Yes 0:37	Yes 0:39	Yes 0:38	*	No	*	*
Sinkhole E	09/25/97 11:04	Flourescein	25 ml	*	*	*	*	*	No	Yes 0:06	Yes?	Yes 0:07
Sinkhole F	09/23/97 10:34	Flourescein	100 ml	*	Yes? ??:??	*	*	*	Yes 21:29	Yes 5:46	Yes 10:00	Yes 1:25
Sinkhole F	10/15/97 13:05	Flourescein	1 l	*	Yes? 7 days	*	*	Yes 7 days	*	Yes 3:55	Yes 4:54	Yes 4:57

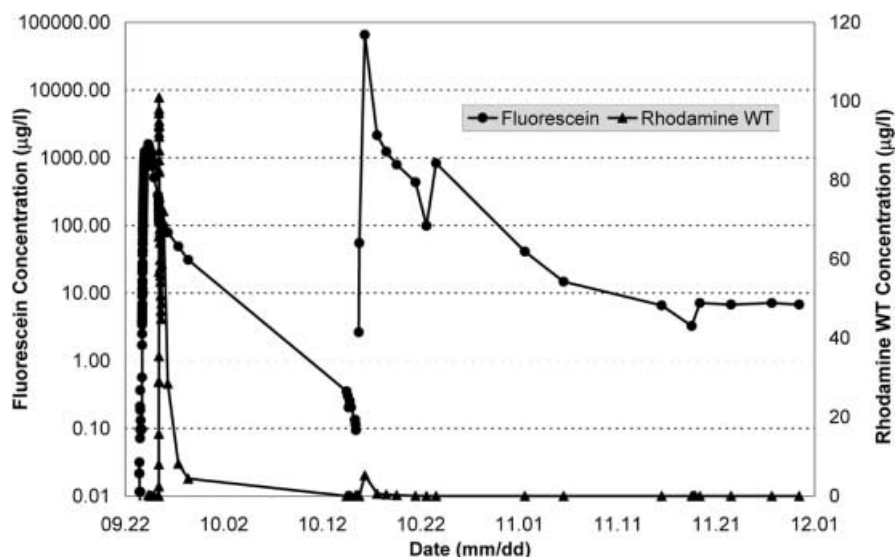


**Fig. 4**  
Dye breakthrough curves at QRS

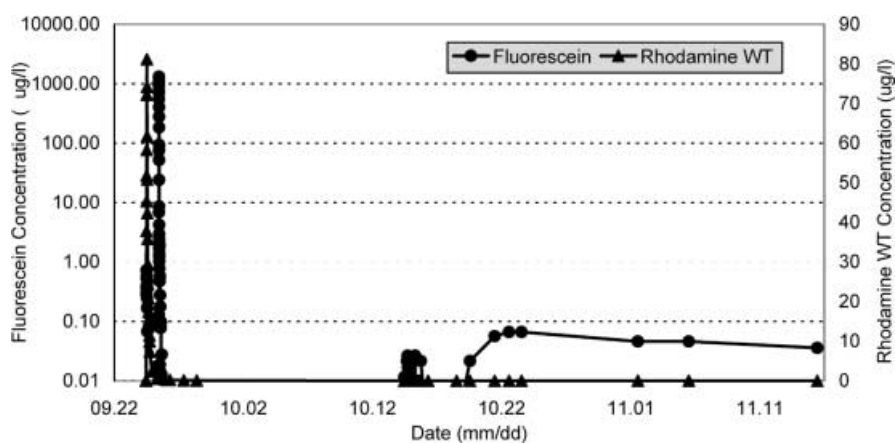


**Fig. 5**  
Dye breakthrough curves at QNS

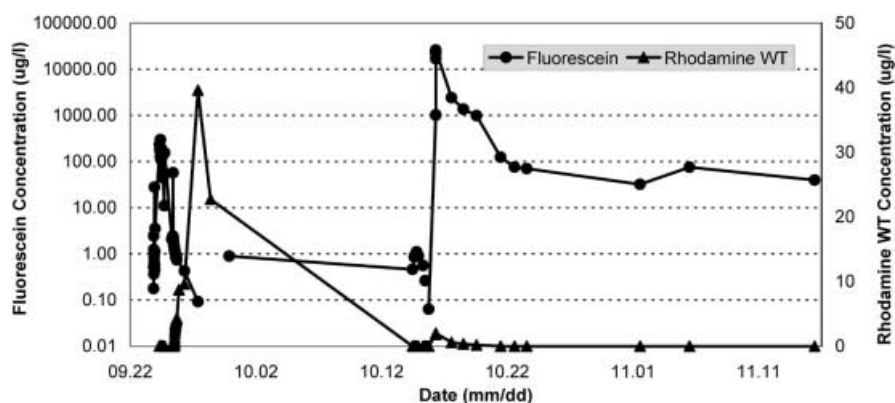


**Fig. 6**  
Dye breakthrough curves at QBS

concentration of 0.7  $\mu\text{g/l}$ . Because this peak occurred before the insertion of dye into sinkhole E, it was interpreted to result from the dye insertion at sinkhole F on September 23. This interpretation was confirmed by injecting 1 l of fluorescein into sinkhole F on October 15, 1997, which resulted in a breakthrough curve with the peak concentration of 0.066  $\mu\text{g/l}$ . The rhodamine WT peaks at QNS are classic dye breakthrough curves with the

first resulting from dye insertion into sinkhole C and the second from dye insertion into sinkhole B. Although the peaks at QBS are relatively erratic, quantitative dye analysis provided credible evidence that shows its connection to sinkholes B and C. A rhodamine WT peak (1.9  $\mu\text{g/l}$ ) that occurred on September 16 appears to be the result from dye insertion into sinkhole D. Careful laboratory analysis indicated that this peak is



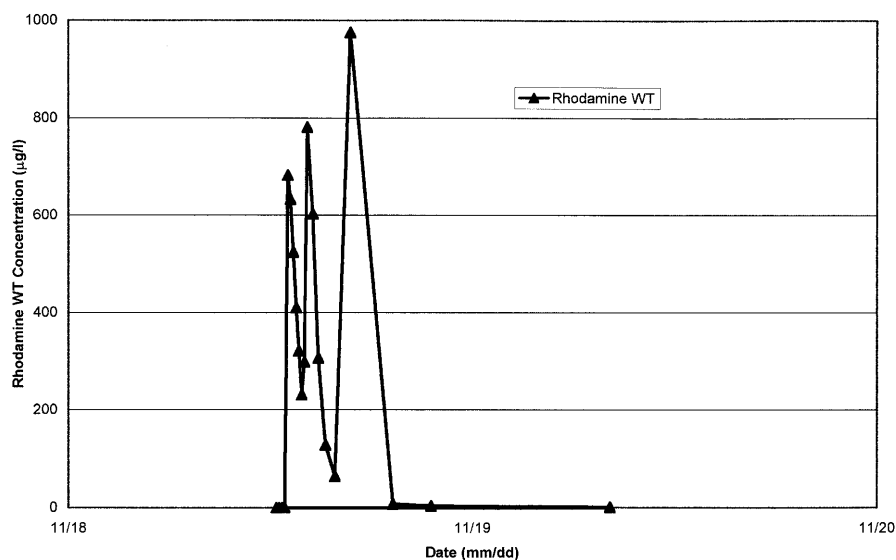


**Fig. 9**  
Dye breakthrough curves at RLB-3

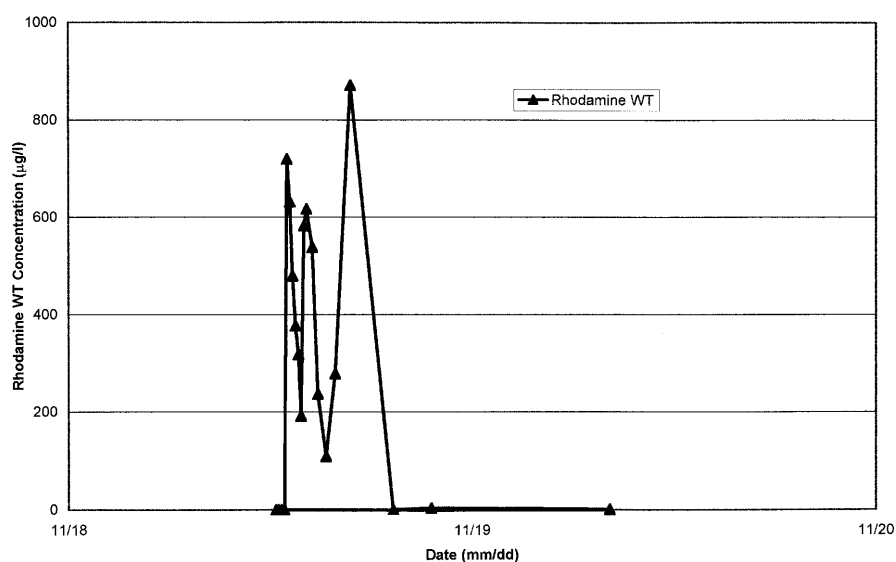


**Fig. 10**  
Dye breakthrough curves at RLB-4

its introduction at sinkhole D, as shown in the close-up graph in Fig. 8. The double peaks indicate that the dye entered the stream in conjunction with two water insertions at sinkhole D. Although the absolute concentration of rhodamine WT was very low, less than  $2 \mu\text{g/l}$ , the pattern that the breakthrough curve displayed supports positive detection of the dye. Because the dye was not detected at any other monitoring location, it was hypothesized that the dye had been discharged through a previously unidentified feature in the stream channel. To locate the suspected discharge point, 3.8 l of rhodamine WT was introduced into sinkhole D at a later date. This relatively large amount of dye was used to ensure that its emergence into the stream would be visible. Approximately 30 min after the dye was inserted, it was observed flowing into the stream via two adjacent features. These features are referred to as GrS (Fig. 2). They are at the intersection of a prominent joint and a bedding-plane parting, both of which have been enlarged by dissolution. The discharge of dye from GrS is also documented by

the dye breakthrough curves from three downstream monitoring locations, including RLB-3 and RLB-4 (Figs. 9 and 10). Their individual peaks result from water insertions at sinkhole D and variations in the flow of RLB caused by discharges from a municipal sewage plant. No dye was detected at RLB-5. During the course of the tracer tests, charcoal receptors “dye bugs” were placed at over 50 other locations surrounding the site. The eluant samples from the dye bugs were analyzed by spectrofluorophotometer at the Indiana University and no positive dyes were detected.

## Conclusions

Data collected during this investigation confirms that water entering sinkholes adjacent to the site is predominantly discharged at QRS, QNS, and QBS. The application of a well-planned sampling strategy and a thorough anal-

ysis of the data resulted in the identification of one undiscovered groundwater discharge feature – GrS, which is submerged in the stream adjacent to the site. This feature could not have been identified readily during a typical inventory of karst features. Therefore, groundwater monitoring at the site can be conducted most appropriately at these natural discharge springs. Monitoring stations have been established at QRS and QNS with approval of the relevant regulatory agency. Concentration-dependent sampling and on-site analysis allowed the collection of high-resolution data regarding the flow from multiple sinkholes within a relatively short period of time. Positive dye detection may not rely on the absolute concentration of the injected dye but on a statistically valid breakthrough curve.

## References

- Ash DW (1980) Karst development in the Mitchell Plain and adjacent Crawford Upland in response to lithologic, structural, and hydrologic constraints. Geological Society of America, North-Central Section, 14th Annual Meeting, Bloomington, Indiana, 10–11 April, Abstracts with Programs, vol 12, part 5, p 218
- Atkinson TC, Smart PL (1981) Artificial tracers in hydrogeology. In: A survey of British hydrogeology 1980. The Royal Society, London, pp 173–190
- Ault CH (1993) Map of Indiana showing elevations or thickness of overburden on selected rock units containing thick deposits of limestone and dolomite. Indiana Geological Survey, Miscellaneous Map 56, 1:500,000 scale
- Broermann J, Bassett RL, Weeks EP, Borgstrom M (1997) Estimation of  $\alpha_L$ , velocity,  $K_d$  and confidence limits from tracer injection test data. *Ground Water* 35(6):1066–1076
- Brown MC, Wigley TML (1969) Simultaneous tracing and gaging to determine water budgets in inaccessible karst aquifers. In: Proceedings of the 5th International Congress Speleology, vol 5, Hydrologie des Karstes, Hy 3/1–3/5
- Currens JC (1995) Mass flux of agricultural nonpoint-source pollutants in a conduit-flow-dominated karst aquifer, Logan County, Kentucky. In: Beck BF (ed) Karst geohazards. A.A. Balkema, Rotterdam, pp 179–187
- Dreiss SJ (1989) Regional scale transport in a karst aquifer. *Water Resour Res* 25(1):126–134
- Eckenfelder Inc (1996) Guidelines for wellhead and springhead protection area delineation in carbonate rocks. US Environmental Protection Agency, Region 4, Atlanta, Georgia
- Fenneman NM (1938) Physiography of the eastern United States. McGraw-Hill, New York
- Frushour SS, Harper D, Dintaman C (1997) Dye-trace experiments in the karst region of Indiana: series of seven maps at various scales. Indiana Geological Survey
- Hall RD (1973) Stratigraphy and sedimentation of a sinkhole in south central Indiana. Geological Society of America, North-Central Section, 7th Annual Meeting, Abstracts with Programs, vol 5, part 4, p 319
- Hall RD (1976a) Investigations of sinkhole stratigraphy and hydrogeology, south-central Indiana. *Bull Nat Speleol Soc* 38:88–92
- Hall RD (1976b) Stratigraphy and origin of surficial deposits in sinkholes in south-central Indiana. *Geology* 4(8):507–509
- Hatheway AW (1996) “Karstic” may not be karst; when is it “safe” for a landfill?. *Am Eng Geol News* 39(2), Perspectives No. 21
- Hughes TH, Memon BA, LaMoreaux PE (1994) Landfills in karst terrains. *Bull Assoc Eng Geol* 29(2):203–208
- Johnson PA, Gomez B (1994) Cave levels and cave development in the Mitchell Plain following base-level lowering. *Earth Surf Proc Landf* 19(6):517–524
- Jones WK (1984) Analysis and interpretation of data from tracer tests in karst areas. *Bull Nat Speleol Soc* 46:41–47
- Kasnavia T, Vu V, Sabatini DA (1998) Fluorescent dye and media properties affecting sorption and tracer selection. *Ground Water* 37(3):376–381
- Kass W (1998) Tracing technique in geohydrology. A.A. Balkema, Rotterdam
- Lehmann H (1975) On the morphology of the Mitchell Plain and the Pennyroyal Plain of Indiana and Kentucky (translated from the German by Eberhard Werner). *Cave Geol (State College, Pennsylvania)* 1(2):29–39
- Malott CA (1919) The American bottoms region of eastern Greene County, Indiana. *Indiana University Studies* 40
- Malott CA (1945) Significant features of the Indiana karst. *Proc Indiana Acad Science* 54:8–24
- McConnell H, Horn JM (1972) Probabilities of surface karst-applications in Mitchell Plain, Indiana. In: Spatial analysis in geomorphology. Methuen, London, pp 111–133
- Mull DS, Liebermann TD, Smoot JL, Woosley LH (1988) Application of dye-tracing techniques for determining solute-transport characteristics of ground water in karst terranes. US Environmental Protection Agency, EPA 904/6-88-001
- Olson CG, Ruhe RV, Mausbach JJ (1980) The terra rossa limestone contact phenomenon in karst, southern Indiana. *Soil Sci Soc Am J* 44:1075–1079
- Palmer MV, Palmer AN (1975) Landform development in the Mitchell Plain of southern Indiana – origin of a partially karsted plain. *Z Geomorph* 19(1):1–39
- Powell RL (1961) Caves of Indiana. Indiana Geological Survey, Circular 8
- Powell RL (1973) Karst areas of Indiana – the south-central karst area (physiography and development). Guidebook for the 1973 Convention of the National Speleological Society. Indiana Geological Survey, pp 3–6
- Powell RL, Frushour SS, Harper D (1997) Areas of sinkholes and sinking-stream basins with locations of cave openings and springs in central southern Indiana. Indiana Geological Survey, Miscellaneous Map 65, scale 1:250,000
- Quinlan JF (1986) Water-tracing techniques in karst terranes: practical karst hydrogeology with emphasis on groundwater monitoring, a short course. National Water Well Association, Dublin, Ohio
- Quinlan JF (1990) Special problems of ground-water monitoring in karst terranes. In: Nielsen DM, Johnson AI (eds) Ground-water and vadose zone monitoring. American Society for Testing and Materials, Philadelphia, STP 1053, pp 275–304
- Quinlan JF, Alexander EC Jr (1987) How often should samples be taken at relevant locations for reliable monitoring of pollutants from an agricultural, waste disposal, or spill site in a karst terrane? A first approximation. In: Beck BF, Wilson WL (eds) Karst hydrogeology. A.A. Balkema, Rotterdam, pp 277–286
- Rainwater KA, Wise WR, Charbeneau R (1987) Parameter estimation through groundwater tracer tests. *Water Resour Res* 23(10):1901–1910
- Rexroad CB, Gray LM (1979) Geologic story of Spring Mill State Park. State Park Guide 7. Indiana Geological Survey, Bloomington, Indiana
- Ruhe RV (1977) Summary of geohydrologic relationships in the Lost River watershed, Indiana, applied to water use and environment. In: Dilamarter RR, Csallany SC (eds) Hydrologic problems in karst regions. Proceedings of the International Symposium on Hydrologic Problems in Karst Regions, Bowling

- Green, Kentucky, 26–29 April 1976. Western Kentucky University, pp 64–78
- Ryan M, Meiman J (1995) An examination of short-term variations in water quality at a karst spring in Kentucky. *Ground Water* 34(1):23–30
- Smart CC, Ford DC (1982) Quantitative dye tracing in a glacierized alpine karst. *Beit Geol Schweiz – Hydrol* 28(1):191–200
- Stephenson BJ, Zhou WF, Beck BF, Green TS (1999) Highway stormwater runoff in karst areas – preliminary results of basic monitoring and design of a treatment system for a sinkhole in Knoxville, Tennessee. *Eng Geol* 52:51–59
- Viessman W Jr, Lewis GL, Knapp JW (1989) *Introduction to Hydrology*. Harper & Row, New York
- Wicks CM, Hoke JA (2000) Prediction of the quality and quantity of Maramec spring water. *Ground Water* 38(2):218–225
- Zhou WF (2000) Studies of confluent flow in mature karst aquifers using analog models and numerical mixing cell models. In: Sasowsky ID, Wicks CM (eds) *Groundwater flow and contaminant transport in carbonate aquifers*. A.A. Balkema, Rotterdam, pp 157–168
- Zhou WF, Beck BF, Stephenson JB (1999) Investigation of groundwater flow in karst areas using component separation of natural potential measurements. *Environ Geol* 37(1–2):19–25
- Zhou WF, Beck BF, Stephenson JB (2000) Reliability of dipole-dipole electrical resistivity tomography for defining depth to bedrock in covered karst terranes. *Environ Geol* 39(7):760–766